IEEE Access
Multidisciplinary ⋮ Rapid Review ⋮ Open Access Journal

Received 30 January 2024, accepted 17 February 2024, date of publication 27 February 2024, date of current version 4 March 2024.

Digital Object Identifier 10.1109/ACCESS.2024.3371017

RESEARCH ARTICLE

Design of Stair-Climbing Electric Wheelchair With Tri-Spoke Wheel and Supporting Leg

YOUNGSU CHO*, KWANG JOON KIM*, JONGWOO PARK, HYUNUK SEO, HYUNMOK JUNG, BYUNGIN KIM, DONG-IL PARK, JEONGDO AHN, AND CHANHUN PARK

Department of Robotics and Mechatronics, Korea Institute of Machinery and Materials (KIMM), Daejeon 34103, South Korea

Corresponding authors: Jeongdo Ahn (jdahn@kimm.re.kr) and Chanhun Park (chpark@kimm.re.kr)

This work was supported by the Major Project of Korea Institute of Machinery and Materials under Project NK244F.

*Youngsu Cho and Kwang Joon Kim contributed equally to this work.

ABSTRACT Stair climbing is necessary to improve the convenience of electric wheelchairs. An important issue in developing a climbable wheelchair is stability and speed during climbing. In this work, tri-wheel and supporting leg were adopted in the stair climbing method for high speed and stable posture. Based on the mechanical and static analyses of the climbing mechanism, the design method of the wheel cluster system was expressed as equations. These equations were proposed considering the design parameters that ensure the continuity and stability of the climbing motion. Moreover, the collision information between the stairs and the cluster system during the climbing motion was included in those equations. A validation test of the stair climbing mechanism was performed by manufacturing a prototype of 750 (W) x 800(D) x 1,000(H) mm^3 and 120 kg. The experimental verification proved that the electric wheelchair can stably go up and down the stairs under extreme conditions (stair width = 300 mm, stair height = 180 mm) at a speed of 10 steps/min.

INDEX TERMS Electric wheelchair, stair-climbing, tri-spoke, wheel cluster, supporting leg, stable climbing.

I. INTRODUCTION

A wheelchair is a mobility device designed to help people with lower extremity disabilities such as paralysis or amputation, move about. However, as a wheelchair typically consists of two large wheels and a small auxiliary wheel, it can easily be moved on flat ground or low slopes, but it is very difficult to move up/down the stairs, which are common in building entrances. Ascending/descending movement and flat ground movement will enable access to diverse places, improving the quality of life.

To overcome the low stair-movement performance of existing wheelchairs, several studies have been performed on electric wheelchairs wherein an actuator and a climbing mechanism are added for climbing stairs. Electric wheelchairs that move on stairs typically have a combination of a wheel, a track, and a type of wheel cluster combining several small wheels. First, there is an electric wheelchair in the form of an infinite track. Misawa developed an electric wheelchair with a pair of left and right tracks and four auxiliary casters [1]. On flat ground, the assistant pushes the electric wheelchair as if pushing a general manual wheelchair, and on the stairs, the electric wheelchair can move the stairs using the track. The slope of the stairs is measured using a sensor, and the angle of the passenger seat is separately adjusted according to the slope of the stairs. An electric wheelchair capable of moving alone on a track without wheels has also been developed [2], [3]. Depending on the angle of the stairs or the posture of approaching/ escaping the stairs, the angle of the track was adjusted using an auxiliary wheel, or the articulated track was used to secure stable friction between the stairs and the track. It is possible to move on flat ground and stairs alone by the passenger, but on flat ground, the speed of movement is slower than that of wheels and is highly inefficient. Scewo Bro [4] and TopChair S2 [5] are representative track-based commercial electric wheelchairs, driven using general wheels on flat ground, and driven using track on the stairs. These wheelchairs have efficient locomotion on flat ground with wheels and stable performance for traversing stairs using a track; however, they significantly increase the weight and length owing to a track. In addition, a mechanism for adjusting the height or track

The associate editor coordinating the review of this manuscript and approving it for publication was Hongli Dong.

angle to go up the first stairway or down the last stairway is added, resulting in a heavier and more complex structure.

Meanwhile, electric wheelchairs with a wheel cluster consisting of several small wheels and a tri-spoke have been actively studied. A wheel cluster is applied and combined with a rocker-bogie of cleaning robot for overcoming obstacles of building [6], or a mobile platform for rough terrain driving by mounting a pair of wheel clusters, and driving wheels or two pairs of wheel clusters has been studied [7], [8]. A study on a wheeled robot that overcomes an obstacle over twice its own height by inserting an articulated mechanism between six sets of wheel clusters and the main chassis and vice chassis was reported [9]. As described above, the electric wheelchair to which the wheel cluster with outstanding obstacle-overcoming performance is applied drives using small wheels on flat ground similar to the conventional wheels of manual wheelchairs or track-based electric wheelchairs.

To overcome the stairs using the wheel cluster, the design parameters of the tri-spoke and small wheel constituting the wheel cluster must be determined according to the stair dimension. Because only the two small wheels on either side support the wheelchair, complex balancing control is essential to balance the wheelchair when the tri-spoke rotates to overcome the stairs. In addition, a simultaneous trajectory of the small wheel and tri-spoke must be created. Balan et al. designed a wheel cluster that rotates small wheels using gears to overcome stairs [10]. However, as basic-stage research, there is a lack of wheel cluster design process considering the dimension of the stairs, and research on balancing and trajectory generation remains insufficient. Fang et al. developed a wheelchair using a pair of left and right wheel clusters, and an anti-tip-over bracket was applied to this wheelchair to prevent it from overturning while overcoming stairs [11]. Stability was improved by securing the stability margin of stair climbing using this bracket, but the user still cannot climb the stairs alone and needs an assistant's help. Lawn and Ishimatsu combined four sets of wheel clusters with an articulation mechanism to overcome high obstacles such as vans by controlling the wheelchair alone by the passenger. However, owing to complex mechanisms, the overall size of the wheelchair increased, and the structure became complicated [12]. A study on a wheelchair combined the track and wheel cluster. Quaglia et al. proposed a mobile platform that climbs stairs using a track on the back of a wheel-cluster-based wheelchair [13]. By applying the cam mechanism, the passenger's oscillation that occurs when the wheel cluster climbs the stairs is reduced. However, in determining the design parameters of the wheel cluster, the consideration of the stair dimension remains insufficient. Moreover, since this platform combines wheel clusters and tracks, the entire system becomes complex and heavy.

In this study, to increase the stability of a wheel cluster-type electric wheelchair, a supporting leg mechanism was developed for stable support when climbing stairs on the back of the wheelchair. In Section II, a systematic design process for determining wheel cluster parameters was established such as the length and width of the tri-spoke and the diameter of the wheel according to the height and width of the target stairs. Moreover, the trajectory of each actuator including wheel cluster and supporting leg was derived from kinematic analysis, and the static analysis was performed to prevent from overturning the wheelchair when overcoming the stairs. Performance verification experiments and conclusions of the proposed electric wheelchair are presented in Sections IV and V, respectively.

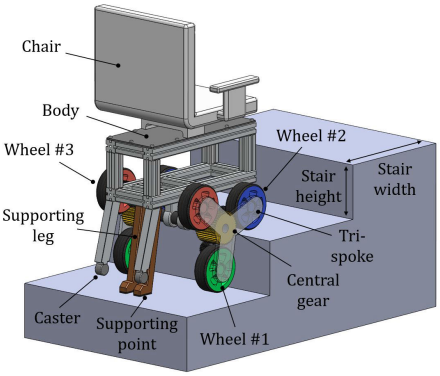

FIGURE 1. Initial climbing posture of the system. Wheel #1 is contacted to the ground & wall and wheel #2 is contacted to the floor of the upper stair.

II. DESIGN OF WHEEL CLUSTER SYSTEM WITH A SUPPORTING LEG

A. DESIGN CONCEPT

The wheel cluster system invented in this study is shown in Fig. 1, wherein the wheel cluster consists of tri-spoke and three wheels, connected to each other by spokes. To initiate the climbing mechanism, two wheels should contact the tread of the stairs, and then climbing proceeds by rotating a spoke and wheels under the contact condition. Several mechanical assisting structures such as legs [14], [15], arms [16], tail [17], [18] were studied for increasing the climbing stability. In this study, leg type was adopted to the cluster system for increasing the climbing stability.

During the climbing process, a collision between the stairs and the system can occur because of the thickness of spokes or the radius of the central gear. To design the system without these collision problems, several design parameters were considered, as shown in Fig. 2.

B. DESIGN PARAMETERS OF WHEEL CLUSTER

To prevent the collision of the system during climbing, the design parameters of the wheel cluster and environmental conditions of the stair are expressed in formulas. In the process of climbing stairs, the angle formed by the lower spoke with the ground is defined as θ_w as shown in (1).

$$\theta_w = arcsin\left(\frac{h_s}{2r_a cos\frac{\pi}{6}}\right) + arccos\left(\frac{r_a cos\frac{\pi}{6}}{r_a}\right) \quad (1)$$

The conditions of climbable stairs with a cluster system are expressed as follows. To secure the system stability, over half

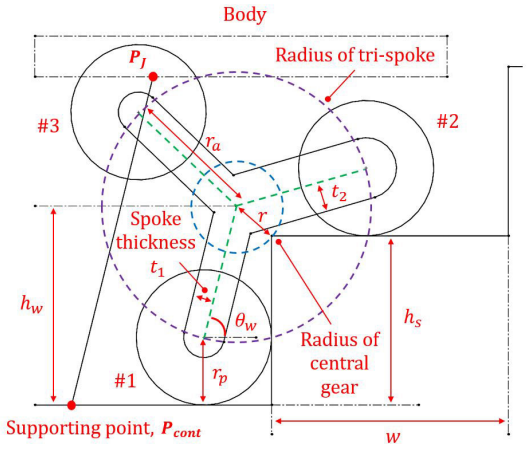

FIGURE 2. Design parameters of the wheel cluster system with supporting leg. (θ = angle between the ground and spoke of wheel #1. r_p = radius of wheel, r_a = length of spoke. t_1 = thickness of spoke of wheel #1. t_2 = thickness of spoke of wheel #2. r = radius of central gear. h_s = height of stair. h_w = height of center of tri-spoke).

of the wheel center must be located on the upper stair, and it is expressed as (2). Moreover, the center distance of two wheels, which are in contact with stairs, should be smaller than the stair width for stability and is expressed in (3).

$$r_a cos\theta_w + r_a cos\left(\theta_w - \frac{\pi}{3}\right) \geq r_p \tag{2}$$

$$r_a cos\theta_w + r_a cos\left(\theta_w - \frac{\pi}{3}\right) \leq w \tag{3}$$

The collision conditions of the wheel spoke thickness (t_1, t_2) and center gear radius (r) are defined using (4) to (6).

$$t_1 = (r_p - r_a cos\theta_w) sin\theta_w + (r_p - r_a sin\left(\theta_w - \frac{\pi}{3}\right)) cos\theta_w \tag{4}$$

$$t_2 = (r_p - r_a cos\theta_w) sin\left(\theta_w - \frac{\pi}{3}\right) + (r_p - r_a sin\left(\theta_w - \frac{\pi}{3}\right)) cos\left(\theta_w - \frac{\pi}{3}\right) \tag{5}$$

$$r = \sqrt{(r_a cos\theta_w - r_p)^2 + (r_p - r_a sin\left(\theta_w - \frac{\pi}{3}\right))^2} \tag{6}$$

Lastly, the maximum climbable height of stair ($h_{s,max}$) is defined using (7) by selected wheel radius (r_p) and spoke length(r_a).

$$h_{s,max} = r_a \sqrt{3} sin\left(arccos\left(\frac{r_p}{r_a\sqrt{3}}\right)\right) \tag{7}$$

The wheel radius of the wheel cluster proposed in this study was limited to 240 to 260 *mm* based on a commercial wheelchair size for convenient daily use. Regularly, the legally mandated height for stairs is approximately 180 *mm* with a tolerance of ± 25% (ranging from 135 to 225 *mm*), while the mandated width is around 300 *mm* with a ± 25% tolerance (ranging from 255 to 345 *mm*). To address this variability in stair dimensions, we calculated the tri-spoke length (r_a) and wheel radius (r_p) of the electric wheelchair. In essence, the capacity of the system to navigate stairs is

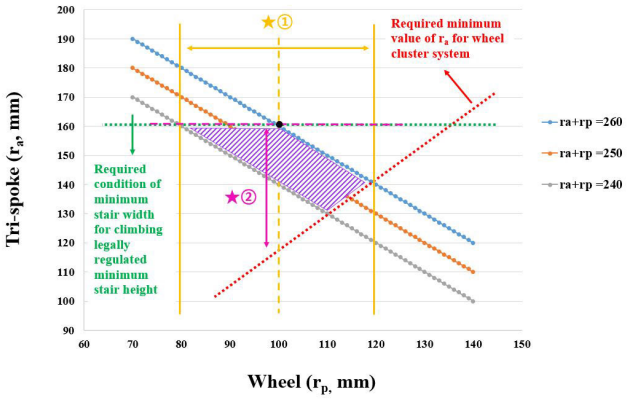

FIGURE 3. Variable value selection process of the wheel radius and spoke length diverse conditions.

contingent on the values of r_a and r_p. These variables have mechanical relationships such as $r_a \leq r_p$ and $r_{p,max} = \frac{\sqrt{3}}{2} r_a$ due to the limitation of the tri-spoke structure. The possible combinations of r_a and r_b can be designed based on these conditions, as shown by the purple area in Fig. 3. If the wheel size (r_p) is small, the maximum climbable height increases, but the driving stability is decreased. Based on this condition, the radius of the wheel was selected as 100 *mm*, which is the middle value between 80 to 120, which is a possible range on the graph. This process is indicated by ① in Fig. 3. Moreover, as shown in (4) and (5), the thickness (t) is proportional to r_a; then a larger thickness is advantageous for securing the installation space. Hence, the maximum value of r_a(160*mm*) was selected in the purple area of the graph to have a maximum spoke thickness for a sufficient installation space. This process is indicated by ② in Fig.3.

C. STAIR CLIMBING MECHANISM

To create a natural trajectory from the discontinuous movements of the wheel cluster system, the climbing process is separated into three steps, as shown in Fig. 4. First, a green wheel climbs the stair vertically under the contact condition. Second, a green wheel rotates along the nosing of the stairs under the point-contact condition. When the blue wheel touches the riser of the upper stair, the final step is initiated, and the tri-spoke rotates until the red wheel touches the tread of the next upper stair.

1) KINEMATICS

To define the mechanical relationships of each step, transverse moving distance and longitudinal moving distance of tri-spoke are defined as Fig. 5. Addition- ally, the amounts of change in control variables of cluster system are expressed in TABLE 1 to define the mechanical relationships of the system.

In the first step, according to the transverse velocity of the tri-spoke($\dot{w_{wi}}$), the mechanical relationships of height velocity of tri-spoke($\dot{h_{wi}}$), rotation velocity of tri-spoke($\dot{\theta_{wi}}$), length velocity of supporting leg($\dot{l_i}$), and rotation velocity of

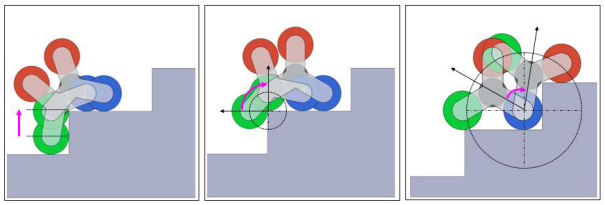

FIGURE 4. Three steps of climbing process. (a) Trajectory of the first step of climbing. (b) Trajectory of the second step. (c) Trajectory of the third step.

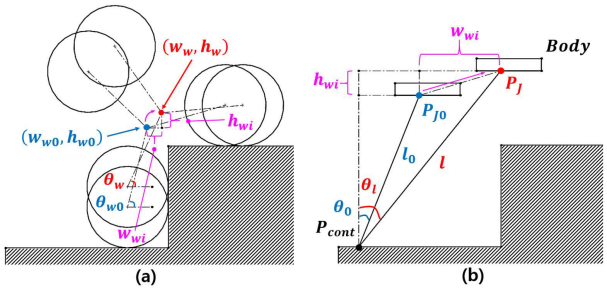

FIGURE 5. Control variables of wheel cluster system with a supporting leg. (a) Control variables of the tri-spoke with three wheels. (b) Control variables of the supporting leg.

TABLE 1. Control variables of the wheel cluster with supporting leg.

	Symbol	Explanation
1	$w_{wi} = w_w - w_{w0}$	Transverse displacement of tri-spoke
2	$h_{wi} = h_w - h_{w0}$	Longitudinal displacement of tri-spoke
3	$\theta_{wi} = \theta_w - \theta_{w0}$	Rotated angle of tri-spoke
4	$l_i = l - l_0$	Changed length of supporting leg
5	$\theta_{li} = \theta_l - \theta_0$	Rotated angle of supporting leg

the supporting leg($\dot{\theta_{li}}$) are defined from (8)-(12). Depending on these mechanical relationships, the posture and position of the wheel cluster system during climbing are determined.

$$\dot{\theta_{wi}} = \frac{\dot{w_{wi}}}{-r_a sin(\theta_{wo} + \theta_{wi})} \tag{8}$$

$$\dot{h_{wi}} = -r_a \dot{\theta_{wi}} cos\left(\theta_{wo} + \theta_{wi} - \frac{\pi}{3}\right) + k_p((h + r_p) - (h_{w0} + h_{wi} + r_a sin\left(\theta_{wo} + \theta_{wi} - \frac{\pi}{3}\right)) \tag{9}$$

$$\dot{l_i} = \frac{1}{(l_i + l_0)} \begin{pmatrix} \dot{w_{wi}} \\ \dot{h_{wi}} \\ 0 \end{pmatrix}^T (\boldsymbol{P}_J \ -\boldsymbol{P}_{cont}) \tag{10}$$

$$\dot{\theta_{li}} = \frac{-sin\theta_l \dot{l_i}}{(l_0 + l_i)cos\theta_l} + \frac{\dot{w_{wi}}}{(l_0 + l_i)cos\theta_l} \tag{11}$$

The mechanical relationships of the second and third steps are expressed below. (12) and (13) express the rotation and height velocities of the tri-spoke in the second step. In 12, θ_{w1} denotes the angle formed by the center of the lower wheel and the tread of the upper stair when the former is located higher than the latter. (14) and (15) represent the rotational and height velocities of the tri-spoke in the third step. The definitions of length velocity ($\dot{l_i}$) and rotation velocity($\dot{\theta_{li}}$) of the supporting leg are the same in all steps.

$$\begin{pmatrix} \dot{w_{wi}} \\ 0 \end{pmatrix} = \begin{pmatrix} r_p sin\theta_{w1} & -r_a sin(\theta_{w0} + \theta_{wi}) \\ r_p cos\theta_{w1} & r_a\sqrt{3}cos\left(\theta_{w0} + \theta_{wi} - \frac{\pi}{6}\right) \end{pmatrix} \begin{pmatrix} \dot{\theta_{w1}} \\ \dot{\theta_{wi}} \end{pmatrix} \tag{12}$$

$$\dot{h_{wi}} = -r_a cos\left(\frac{\pi}{3} - \theta_{w0} - \theta_{wi}\right)\dot{\theta_{wi}} + k_p((h + r_p) - (h_{wo} + h_{wi} - r_a sin\left(\frac{\pi}{3} - \theta_{w0} - \theta_{wi}\right))) \tag{13}$$

$$\dot{\theta_{wi}} = \frac{\dot{w_{wi}}}{-r_a sin\left(\frac{\pi}{3} - (\theta_{w0} + \theta_{wi})\right)} \tag{14}$$

$$\dot{h_{wi}} = -r_a cos\left(\frac{\pi}{3} - \theta_{w0} - \theta_{wi}\right)\dot{\theta_{wi}} + k_p((h + r_p) - (h_{wo} + h_{wi} - r_a sin\left(\frac{\pi}{3} - \theta_{w0} - \theta_{wi}\right))) \tag{15}$$

TABLE 2 denotes the initial, running, and terminal conditions for each three steps. Fig. 6 shows a series of control processes of the wheel cluster system.

2) STATICS

For a wheelchair to climb, the most important issue is safety. All configurations during climbing must guarantee static equilibrium to prevent it from flipping. Because several contact points exist during climbing, many linear combinations of ground reaction forces are needed for equilibrium. However, it does not guarantee that the ground reaction force is physically realizable, i.e., if the ground reaction force acting as holding the mechanism or horizontal force is stronger than the vertical force. Thus, this section shows the statics for this mechanism, based on which, optimal design factors are needed to select an actuator, which is physically realizable.

Here, three cases exist, as shown in Fig. 4. Two of them are in static equilibrium by three contact points (Fig. 4(a) and (b)). The other one is by two contact points (Fig. 4).

For the first two cases, if the wheel cluster is in static equilibrium, the gravitational force is equal to the total ground reaction force acting on the contact points.

$$\boldsymbol{F}_l + \boldsymbol{F}_{w1} + \boldsymbol{F}_{w2} - (m_w + m_{wf} + m_b + m_l)\boldsymbol{g} = 0 \tag{16}$$

where, $\boldsymbol{F}_l$, $\boldsymbol{F}_{w1}$, and $\boldsymbol{F}_{w2}$ are reaction forces acting on $\boldsymbol{P}_{cont}$, $\boldsymbol{P}_{w1}$, and $\boldsymbol{P}_{w2}$, respectively as shown in Fig. 7. m_w, m_{wf}, m_b, and m_l are weight of wheel, tri-spoke, body, and leg, respectively. Here, the linear force f_l along to axial direction of the leg $\hat{\boldsymbol{l}} = \left(l\cos(\theta_l + \pi/2),\ l\cos(\theta_l + \pi/2),\ 0\right)^T$ for the reaction force $\boldsymbol{F}_l$ would be

$$\hat{\boldsymbol{l}}^T \boldsymbol{F}_l - f_l - m_{l1}\hat{\boldsymbol{l}}^T \boldsymbol{g} = 0 \tag{17}$$

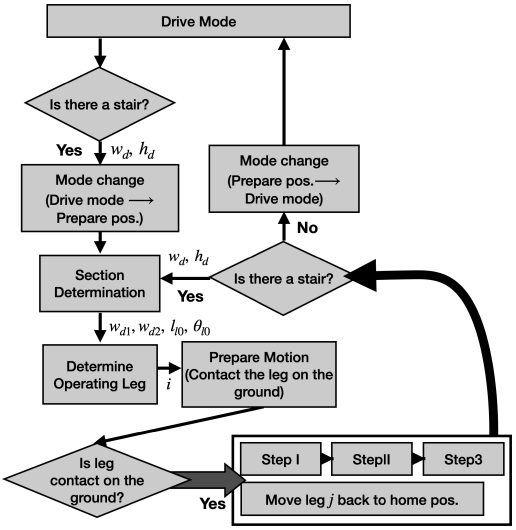

FIGURE 6. A series of control processes to climb the stairs when a moving wheel cluster encounters stairs. The stair information is inputted as w_d and h_d, and the sections with respect to width, w_{d1} and w_{d2}, are determined as shown in Fig. 4(a), (b) and (c).

TABLE 2. Progress condition of each step based on the position.

	Stage	Condition
Step I	Initiation	$h-(r_a sin\left(\theta_w-\frac{\pi}{3}\right)+r_a sin\theta_w)=0$
Step I	Run	$h-(r_a sin\left(\theta_w-\frac{\pi}{3}\right)+r_a sin\theta_w)<h-r_p$
Step I	Termination	$h-(r_a sin\left(\theta_w-\frac{\pi}{3}\right)+r_a sin\theta_w)=h-r_p$
Step II	Initiation	$h-(r_a sin\left(\theta_w-\frac{\pi}{3}\right)+r_a sin\theta_w)=h-r_p$
Step II	Run	$r_a cos\left(\frac{\pi}{3}-\theta_w\right)+r_a cos\theta_w-r_p cos\theta_{w1}+r_p<w$
Step II	Termination	$r_a cos\left(\frac{\pi}{3}-\theta_w\right)+r_a cos\theta_w-r_p cos\theta_{w1}+r_p=w$
Step III	Initiation	$r_a cos\left(\frac{\pi}{3}-\theta_w\right)+r_a cos\theta_w-r_p cos\theta_{w1}+r_p=w$
Step III	Run	$r_a sin\left(\frac{\pi}{3}+\theta_w\right)+r_a sin\left(\frac{2\pi}{3}+\theta_w\right)+r>h+r$
Step III	Termination	$r_a sin\left(\frac{\pi}{3}+\theta_w\right)+r_a sin\left(\frac{2\pi}{3}+\theta_w\right)+r=h+r$

In addition, for static equilibrium, the sum of moments acting on the center of mass of the body also equals to zero as

$$\tau_b+\tau_{F,l}-\tau_l+\tau_{F,wf}-\tau_{wf}+\tau_m=0 \tag{18}$$

where $-\tau_l$ and $-\tau_{wf}$ are the reaction torques made from leg and wheel frame torque, respectively. $\tau_{F,l}$ and $\tau_{F,wf}$ are torques generated by the reaction force from the ground contact. τ_m is generated by the loaded mass. These torques are given as

$$\tau_l=-\hat{z}^T\left((\boldsymbol{P}_c-\boldsymbol{P}_j)\times\boldsymbol{F}_l\right) \tag{19}$$
$$\tau_{F,l}=\hat{z}^T((\boldsymbol{P}_J-\boldsymbol{P}_{com})\times\boldsymbol{F}_J) \tag{20}$$
$$\tau_{F,wf}=\hat{z}^T((\boldsymbol{P}_w-\boldsymbol{P}_{com})\times\boldsymbol{F}_w) \tag{21}$$
$$\tau_m=\hat{z}^T\left((\boldsymbol{P}_m-\boldsymbol{P}_{com})\boldsymbol{g}\right) \tag{22}$$

where $\boldsymbol{F}_J$ is the reaction force acting on $\boldsymbol{P}_J$ to the body, it equals $\boldsymbol{F}_l-m_{l1}g$, and $\boldsymbol{F}_w$ is

$$\boldsymbol{F}_w=\boldsymbol{F}_{w1}+\boldsymbol{F}_{w2}-(m_w+m_{wf})\boldsymbol{g} \tag{23}$$
$$\tau_{wf}=\hat{z}^T(((\boldsymbol{P}_{w1}-\boldsymbol{P}_w)\times\boldsymbol{F}_{w1})+((\boldsymbol{P}_{w2}-\boldsymbol{P}_w)\times\boldsymbol{F}_{w2})-((\boldsymbol{P}_{w3}-\boldsymbol{P}_w)\times m_w\boldsymbol{g})) \tag{24}$$

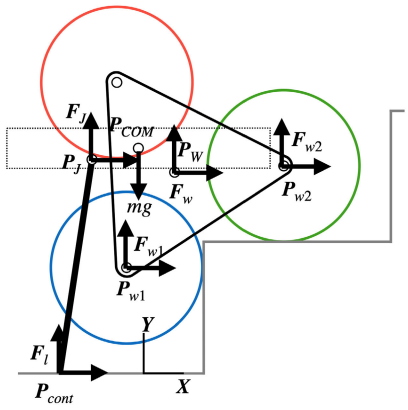

FIGURE 7. Reaction forces acting on wheel cluster system.

The only difference between the two cases is contact configuration. If two wheels contact stair edges, the wheel torque has the following equilibrium condition.

$$r_pF_{w1,y}+r_pF_{w2,x}+\tau_w-r_pm_wg=0 \tag{25}$$

If one wheel is in the corner, its torque has the following equilibrium condition.

$$\hat{z}^T\left(\begin{pmatrix}r_p\cos(-\theta_{w1})\\ r_p\sin(-\theta_{w1})\\ 0\end{pmatrix}\times\left(\boldsymbol{F}_{w1}-\begin{pmatrix}0\\ m_wg\\ 0\end{pmatrix}\right)\right)+r_p\boldsymbol{F}_{w2,x}+\tau_w=0 \tag{26}$$

Correlated statics can be formed by combining (16) to (24) with (25) or (26) according to the contact condition of the wheels as

$$\boldsymbol{A}_1\boldsymbol{x}_1=\boldsymbol{b}_1 \tag{27}$$

where $\boldsymbol{A}_1\in\mathbb{R}^{8\times10}$, $\boldsymbol{b}_1\in\mathbb{R}^{8\times1}$ and the generalized variables can be expressed as

$$\boldsymbol{x}_1=\left(\boldsymbol{F}_{w1}^T,\ \boldsymbol{F}_{w2}^T,\ \boldsymbol{F}_l^T,\ f_l,\ \tau_l,\ \tau_{wf},\ \tau_w.\right)^T\in\mathbb{R}^{10\times1} \tag{28}$$

For the other case, because wheel #1 is not in contact, the force moment equilibrium condition at the ground, tri-spoke wheel, and wheelchair base would be

$$\boldsymbol{F}_l+\boldsymbol{F}_{w2}+(m_b+m_m+m_{wf}+2m_w)\boldsymbol{g}=0 \tag{29}$$
$$\boldsymbol{F}_w=\boldsymbol{F}_{w2}-(2m_w+m_{wf})\boldsymbol{g} \tag{30}$$
$$\tau_{wf}=-\hat{z}^T(((\boldsymbol{P}_{w1}-\boldsymbol{P}_w)\times m_w\boldsymbol{g})+((\boldsymbol{P}_{w2}-\boldsymbol{P}_w)\times\boldsymbol{F}_{w2})-((\boldsymbol{P}_{w3}-\boldsymbol{P}_w)\times m_w\boldsymbol{g})) \tag{31}$$

Statics of this case can be formed from (29) to (31) and from (19) to (22) as

$$\boldsymbol{A}_2\boldsymbol{x}_2=\boldsymbol{b}_2 \tag{32}$$

where $\boldsymbol{A}_2\in\mathbb{R}^{7\times8}$, $\boldsymbol{b}_2\in\mathbb{R}^{7\times1}$ and generalized variables can be expressed as

$$\boldsymbol{x}_2=\left(\boldsymbol{F}_{w2}^T,\ \boldsymbol{F}_l^T,\ f_l,\ \tau_l,\ \tau_{wf},\ \tau_w\right)^T\in\mathbb{R}^{8\times1} \tag{33}$$

Because of the redundancy in equilibrium by force distribution, there is a problem regarding the force distribution

for ensuring the safety of this mechanism or determining what actuators are appropriate for operating this mechanism. In addition, although several force distribution sets exist, if the results cannot satisfy physical reality, force distribution may not be the solution. To determine this force distribution, the following optimization problem must be considered for the configuration with two wheels contacting the ground.

$$\min_{\boldsymbol{x}_1} (\boldsymbol{W}_1\boldsymbol{x}_1)^T(\boldsymbol{W}_1\boldsymbol{x}_1) \tag{34}$$

$$\text{subject to } \mu \boldsymbol{F}_{l,y} > ||\boldsymbol{F}_{l,x}|| \tag{35}$$

$$-\mu \boldsymbol{F}_{w1,x} > ||\boldsymbol{F}_{w1,y}|| \tag{36}$$

$$\mu(\boldsymbol{F}_{w2,y} + m_w g) > ||\boldsymbol{F}_{w2,x}|| \tag{37}$$

where $\boldsymbol{W}_1$ is the weight function; (35), (36), and (37) represent non-slip conditions for each contact point. $\boldsymbol{x}_1$ is formed following general solution with linear combination from the null basis $\boldsymbol{N}_1$ of $\boldsymbol{A}_1$ as

$$\boldsymbol{x}_1 = \boldsymbol{A}_1^{\dagger}\boldsymbol{b}_1 + \boldsymbol{N}_1\boldsymbol{\lambda}_1 \tag{38}$$

Likewise, the following optimization problem is for the configuration that one wheel contacts ground.

$$\min(\boldsymbol{W}_2\boldsymbol{x}_2)^T(\boldsymbol{W}_2\boldsymbol{x}_2) \tag{39}$$

$$\text{subject to (35)} \tag{40}$$

$$\boldsymbol{F}_{2,x} < 0 \tag{41}$$

$$\boldsymbol{F}_{2,y} > 0 \tag{42}$$

Because the wheel is at the stair corner, if all reaction force directions acting on the wheel come from the ground as in (41) and (42), the condition becomes physically reasonable.

The center of mass of the total system should be considered. The wheel cluster system changes its configuration during stair climbing, implying that contact points are changed. In statics, if the total system's center of mass exceeds its contact boundary, no possible solution exists. Thus, a design wheel cluster system with an appropriate center of mass must be designed, ensuring that the center of mass is located between the contact points for all configurations.

III. EXPERIMENTS AND RESULTS

To achieve the stair climbing locomotion presented above, the various parameters should be properly determined. In this section, we present the mechanical design of the cluster system and experiment results. The design and static parameters of the wheel cluster system were determined based on extreme stair climbing conditions.

Fig. 8 shows the main components of our wheel-cluster-type electric wheelchair, wheel cluster (Fig. 8(a)), and supporting leg (Fig. 8(b)). As explained in Section II, an electric wheelchair can drive and climb stairs using the wheel cluster mechanism and support leg. There are two rotational motors to actuate the wheel and tri-spoke. The rotation of the wheel actuating motor is transferred through the belt and spur gears and eventually rotates the wheels. Therefore, three wheels

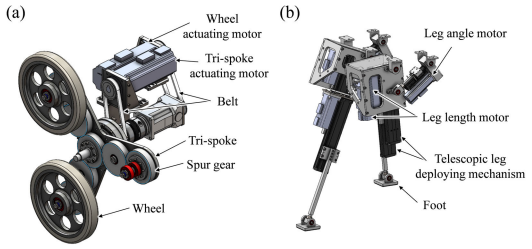

FIGURE 8. Main component of the wheel cluster-type electric wheelchair. (a) Wheel cluster and (b) supporting leg.

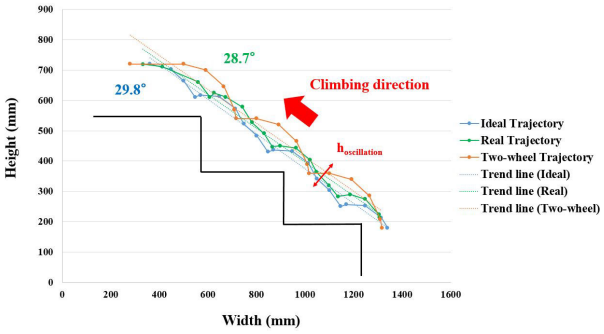

FIGURE 9. Climbing trajectory of ideal (blue line), real (green line), and two wheel system (orange) with a linear regression trend line.

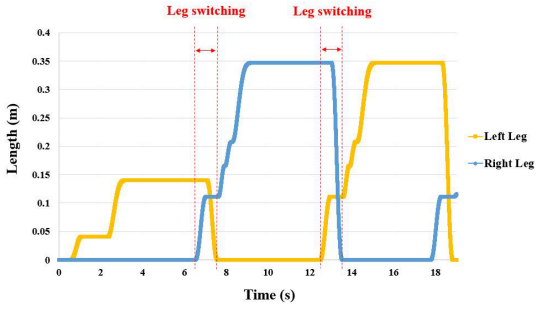

FIGURE 10. Length change of supporting legs with switching mechanism for stable stair climbing.

TABLE 3. Comparison between wheel cluster system and other studies.

	Type	Climbing speed	Driving speed	Weight	Size (W x D x H, mm)
Proposed	3wheels cluster and supporting leg	10 $step/min$	9.0 km/h	120 kg	750 x 800 x 1100
R. Morales et al. [19]	Height adjustable front and rear axles	3 $step/min$	2.0 km/h	90 kg	620 x 1000 x 1100
S. Nakajima [20]	4 driven wheels with steering	2.4 $step/min$	5.4 km/h	70 kg	739 x 800 x 1230
K. R. Cox [21]	3 wheels on spider wheel and rear skids	2.4 $step/min$	8.0 km/h	111 kg	552 x 890 x 900
J. Yuan et al. [22]	8 vertical prismatic joints and 8 wheels	8 $step/min$	1.5 km/h	46 kg	622 x 1050 x 602

rotate with the same velocity and direction. The rotation of tri-spoke actuating motor is transferred through the belt, and it rotates the tri-spoke. By rotating wheels and tri-spoke, the electric wheelchair drives and climbs the stairs according to the generated trajectory.

Meanwhile, a supporting leg mechanism is used for stable support during climbing stairs on the back of the

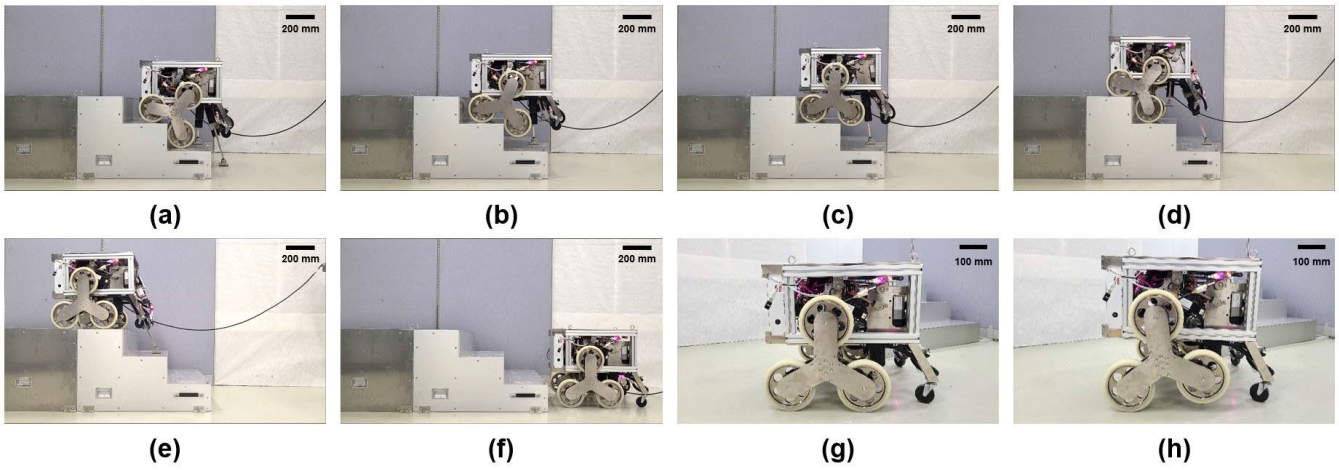

FIGURE 11. Various postures of the wheel cluster system during climbing, descending, and driving. (a) Initiate posture of 1st step (b) Initiate posture of 2nd step. (c) Initiate posture of 3rd step. (d) Terminate posture of 3rd step. (e) Posture after climbing the stairs. (f) Posture after descending stairs. (g) Preparation mode. (h) Driving mode.

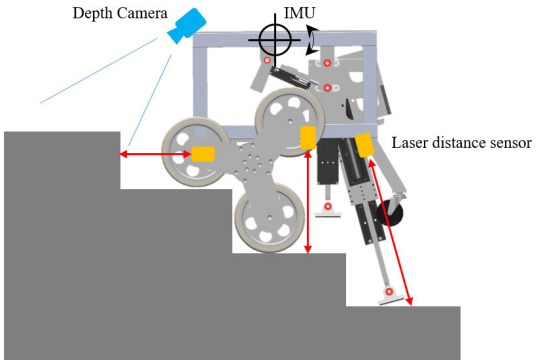

FIGURE 12. Sensors and installation locations to be used in sensor fusion-based climbing control algorithm.

electric wheelchair. Two supporting legs are implemented, and each leg alternately supports the electric wheelchair. The supporting leg can change the leg angle from 0 to 30 deg. using the leg angle motor. In addition, owing to the telescopic leg deploying mechanism using two leg-length motors, the leg length can be quickly adjusted and the total length when contracted is short. Particularly, the motor and ball screw used in the telescopic leg deploying mechanism are selected to lift the entire load (200 kg) of the electric wheelchair and passengers with one supporting leg in a static environment.

Moreover, to mitigate the risk of slipping during stair traversal, urethane wheels were employed, and a patterned rubber pad was integrated on the underside of the supporting legs to enhance friction with the stairs.

The size of the main body of the electric wheelchair was 750(W) x 800(D) x 1,000(H) mm^3 and the mass was approximately 120 kg. Based on the static analysis performed in Section II, the actuators were selected as follows. For the control of tri-spoke and wheel rotation, four motors from KOMOTEK Institute, Korea (KAFZ-04DW6B21, 400 W, 1.3 Nm) were employed. Additionally, four motors (KAFZ02DW6B21, 200 W, 0.64 Nm) were utilized for supporting leg length control, while two motors (KAFZ-01DW6B21, 100 W, 0.32 Nm) were dedicated to angle control.

A prototype of an electric wheelchair was tested for verifying the performance of the system with three-step stairs. The condition of the test stair was based on the Korean building regulation (stair width = 300 mm, stair height = 180 mm). The angle between the linear regression trend line of the ideal climbing trajectory and the ground was approximately 29.8 degrees, and the real climbing trajectory 28.7 degrees, as shown in Fig. 9. As the ideal and real trajectories coincided, the climbing system operated as intended. In addition, the gradient of the climbing trajectory and the stair coincided, implying the progression of stable climbing. Moreover, the wheel cluster mechanism resulted in a 27.3% reduction in climbing oscillation, decreasing it from 101 to 73.3 mm as compared to the two-wheel system. This reduction in climbing trajectory oscillation suggests a potential improvement in passenger comfort.

TABLE 3 shows the comparison between the proposed electric wheelchair of the wheel cluster with a supporting leg system and those in previous studies [19], [20], [21], [22]. The primary function of an electric wheelchair is mobility, and the proposed electric wheelchair in this study is designed for driving at a speed of 9 km/h on a flat surface. Additionally, it exhibits high stability while ascending stairs at a rate of 10 $steps/min$, facilitated by the use of supporting legs.

To secure stability during the climbing process, the supporting leg is supported on the ground (or the lower tread) before starting the climbing. For climbing the next stair, the grounded supporting leg is switched first and then the climbing process begins. To prevent the flip-over, the supporting leg is not detached from the ground (or the lower tread) until the entire process of climbing or descending is finished. The detailed sequence of leg switching process is shown in Fig. 10. The blue and yellow solid lines represent the change of the supporting legs length.

The various postures of the system, such as climbing and descending, are detailed in Fig. 11. Since the wheel cluster system is designed based on Korean building regulations, it cannot overcome difficult terrains that are higher or narrower than regulations. To overcome the rough and various conditions of obstacles, the structure of the tri-spoke must be redesigned into a deformable structure. Additionally, to upgrade the climbing speed similar to human beings, the operation speed of the supporting leg must be changed as well. However, a higher speed can decrease the system stability and increase the operation noise; thus, an additional optimized speed control method is required for solving these expected problems.

IV. DISCUSSION AND CONCLUSION

In the climbing mechanism of this study, the trajectory of the system was created based on the preset stair information. Through the experimental results, we could confirm that the proposed electric wheelchair system with a climbing mechanism performed a stable stair climb. However, the actual size of the experimental stairs and robot size differ from the ideal size due to manufacturing or assembly errors. If errors in the mechanical parameters of the prototype type used in kinematics analysis or differences in step dimensions occur, the trajectory of the wheel cluster and supporting leg is not accurate, resulting in unwanted motion. When the actual stair height is lower than the value used to generate the trajectory, vibration and noise occur as the supporting leg applies an instantaneous impact to the tread of the stairs. Conversely, when the actual height of the stairs is higher than the calculated height, the supporting leg does not properly support the tread of the stairs, resulting in slipping or tilting of the wheelchair.

We proposed an electric wheelchair system consisting of a tri-spoke and supporting legs for high-speed and stable stair climbing. Critical design parameters were proposed to prevent the collision between the stair nose and the system during the climbing process, and a static analysis was conducted to ensure stable operation while ascending or descending stairs. In addition, based on the kinematic and static analyses, the climbing mechanism using tri-spoke and supporting legs was expressed as a formula, and a method for selecting system specifications was proposed using the same. After manufacturing the prototype, the climbing performance test was conducted in extreme conditions and successfully performed at a climbing speed of 10 steps/min. In conclusion, using the tri-spoke and supporting legs, the obstacle could be overcome at a high speed with excellent stability.

Unfortunately, the current climbing system can only overcome stairs of a predetermined size. Addressing real-time changes in stair dimensions is crucial for enhancing the climbing performance of electric wheelchairs. In future endeavours, we intend to implement a climbing control algorithm based on sensor fusion to better adapt the electric wheelchair system to varying stair conditions. Fig. 12 shows that this algorithm measures the height and width of the stairs using a depth camera and the posture of the wheelchair using a laser distance sensor and an IMU sensor. By generating the trajectory of the wheel cluster and supporting leg based on the measured data, it can respond to the change in the dimension of the stairs and the mechanical error of the wheelchair. Furthermore, we plan to extend our analysis beyond the static examination conducted in this study and delve into dynamic stability analysis. This is particularly essential as dynamic stability during stair traversal directly impacts the overall stability of the system. Moreover, we will develop a system that can overcome higher stairs by changing the fixed-size wheel to a transformable tri-spoke structure where the frame length can be changed.

REFERENCES

[1] R. Misawa, "Stair-climbing vehicle for wheelchair," U.S. Patent 6 536 158, Dec. 12, 2000.
[2] S. R. Thamel, R. Munasinghe, and T. Lalitharatne, "Motion planning of novel stair-climbing wheelchair for elderly and disabled people," in *Proc. Moratuwa Eng. Res. Conf. (MERCon)*, Jul. 2020, pp. 590–595.
[3] B. Sharma, B. M. Pillai, K. Borvorntanajanya, and J. Suthakorn, "Modeling and design of a stair climbing wheelchair with pose estimation and adjustment," *J. Intell. Robotic Syst.*, vol. 106, no. 3, pp. 1–18, Nov. 2022.
[4] R. Haridy. (2017). *Stylish Stair-Climbing Wheelchair Merges the Segway With a Tank*. [Online]. Available: https://newatlas.com/scewo-stair-climbing-wheelchair/48653/
[5] A. Heinrich. (2016). *Topchair-S Wheelchair Has no Problem With Stairs*. [Online]. Available: https://newatlas.com/topchair-s-stair-climbing-wheelchair/41421/
[6] J. Hong, G. Park, J. Lee, J. Kim, H. Soo Kim, and T. Seo, "Performance comparison of adaptive mechanisms of cleaning module to overcome step-shaped obstacles on Façades," *IEEE Access*, vol. 7, pp. 159879–159887, 2019.
[7] L. M. Smith, R. D. Quinn, K. A. Johnson, and W. R. Tuck, "The tri-wheel: A novel wheel-leg mobility concept," in *Proc. IEEE/RSJ Int. Conf. Intell. Robots Syst. (IROS)*, Sep. 2015, pp. 4146–4152.
[8] A. M. Mya Thu, T. Z. Soe, and T. Okada, "Dynamic analysis for both rolling and climbing of tri-star wheeled robot," *IOSR J. Mech. Civil Eng.*, vol. 13, no. 5, pp. 52–62, May 2016.
[9] Y. Yang, H. Qian, X. Wu, G. Xu, and Y. Xu, "A novel design of tri-star wheeled mobile robot for high obstacle climbing," in *Proc. IEEE/RSJ Int. Conf. Intell. Robots Syst.*, Oct. 2012, pp. 920–925.
[10] B. Balan, D. Sivakumar, K. Murali, M. L. Niranjan, and R. Marthandam, "Stair climbing robot using star-wheel methodology," *Int. J. Recent Technol. Eng.*, vol. 7, pp. 1864–1866, Apr. 2019.
[11] L. Fang, T. Lu, W. He, and K. Yuan, "Dynamic and tip-over stability analysis of a planetary wheeled stair-climbing wheelchair," in *Proc. IEEE Int. Conf. Mechatronics Autom.*, Aug. 2012, pp. 2541–2546.
[12] M. J. Lawn and T. Ishimatsu, "Modeling of a stair-climbing wheelchair mechanism with high single-step capability," *IEEE Trans. Neural Syst. Rehabil. Eng.*, vol. 11, no. 3, pp. 323–332, Sep. 2003.
[13] G. Quaglia, W. Franco, and M. Nisi, "Kinematic analysis of an electric stair-climbing wheelchair," *Ingenieria Universidad*, vol. 21, no. 1, pp. 27–48, Dec. 2016.
[14] T. Mabuchi, T. Nagasawa, K. Awa, K. Shiraki, and T. Yamada, "Development of a stair-climbing mobile robot with legs and wheels," *Artif. Life Robot.*, vol. 2, no. 4, pp. 184–188, Dec. 1998.
[15] B. Seo, H. Kim, M. Kim, K. Jeong, and T. Seo, "FlipBot: A new field robotic platform for fast stair climbing," *Int. J. Precis. Eng. Manuf.*, vol. 14, no. 11, pp. 1909–1914, Nov. 2013.
[16] P. Liu, J. Wang, X. Wang, and P. Zhao, "Optimal design of a stair-climbing mobile robot with flip mechanism," *Adv. Robot.*, vol. 32, no. 6, pp. 325–336, Mar. 2018.
[17] Y. Kim, J. Kim, H. S. Kim, and T. Seo, "Curved-spoke tri-wheel mechanism for fast stair-climbing," *IEEE Access*, vol. 7, pp. 173766–173773, 2019.

[18] J. Shin, D. Son, Y. Kim, and T. Seo, "Design exploration and comparative analysis of tail shape of tri-wheel-based stair-climbing robotic platform," *Sci. Rep.*, vol. 12, no. 1, pp. 1–19, Nov. 2022.
[19] R. Morales, A. Gonzalez, V. Feliu, and P. Pintado, "Environment adaptation of a new staircase-climbing wheelchair," *Auto. Robots*, vol. 23, no. 4, pp. 275–292, Sep. 2007.
[20] S. Nakajima, "RT-Mover: A rough terrain mobile robot with a simple leg-wheel hybrid mechanism," *Int. J. Robot. Res.*, vol. 30, no. 13, pp. 1609–1626, Nov. 2011.
[21] K. R. Cox, "Battery powered stair-climbing wheelchair," U.S. Patent 6 829 484, Nov. 26, 2002.
[22] J. Yuan and S. Hirose, "Research on leg-wheel hybrid stair-climbing robot, zero carrier," in *Proc. IEEE Int. Conf. Robot. Biomimetics*, Aug. 2004, pp. 654–659.

YOUNGSU CHO received the B.S., M.S., and Ph.D. degrees from the Department of Control and Instrumentation Engineering, Korea University, Sejong, South Korea, in 2011, 2013, and 2020, respectively. Since 2020, he has been with the Department of Robotics and Mechatronics, Korea Institute of Machinery and Materials (KIMM). His research interests include the analysis and control of tendon-driven manipulators.

KWANG JOON KIM received the B.S. degree in mechatronics engineering from The University of Manchester, Manchester, U.K., in 2014, and the Ph.D. degree in mechanical engineering from Korea University, Seoul, South Korea, in 2022. He is currently a Postdoctoral Researcher with the Department of Robotics and Mechatronics, Korea Institute of Machinery and Materials (KIMM). His research interests include mechanical system design, hydraulic system design, and production technology.

JONGWOO PARK received the M.S. and Ph.D. degrees in control and instrumentation engineering from Korea University, Seoul, South Korea, in 2007 and 2016, respectively. He is currently a Senior Researcher with the Department of Robotics and Mechatronics, Korea Institute Machinery and Materials (KIMM), Daejeon, South Korea. His research interests include the analysis of robot control, integrative system for robot, human hand motion, and its synthesis for engineering purposes.

HYUNUK SEO received the B.S., M.S., and Ph.D. degrees from Konkuk University, Seoul, South Korea, in 2011 and 2020, respectively. He was a Research Engineer with VC Tech, Gunpo, South Korea. He was responsible for developing the motor drivers of EVs and MAGLEV. He has been a Senior Researcher with Korea Institute of Machinery and Materials (KIMM). His current research interest includes the design of robot motor drivers for cooperative robots.

HYUNMOK JUNG received the M.S. degree in mechanical engineering from Chungnam University, Daejeon, South Korea, in 2016. He is currently a Senior Researcher with the Department of Robotics and Mechatronics, Korea Institute Machinery and Materials (KIMM), Daejeon. His research interests include industrial robot systems and manufacturing automation systems.

BYUNGIN KIM received the Ph.D. degree in mechanical engineering from Chungnam University, Daejeon, South Korea, in 2012. He is currently a Managerial Researcher with the Department of Robotics and Mechatronics, Korea Institute Machinery and Materials (KIMM), Daejeon. His research interests include advanced manufacturing systems, industrial robot systems, robot gripper, and precision machinery.

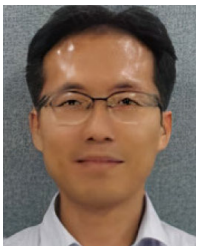

DONG-IL PARK received the B.S., M.S., and Ph.D. degrees in mechanical engineering from Korea Advanced Institute of Science and Technology (KAIST), in 2000, 2002, and 2006, respectively. He has been researching the robotics with Korea Institute of Machinery and Materials (KIMM), since 2006. His research interests include the design, control, and application of robot manipulators and mobile robots.

JEONGDO AHN received the B.S. degree in mechatronics engineering from Korea University of Technology and Education, Cheonan-si, South Korea, in 2012, and the M.S. and Ph.D. degrees in mechanical engineering from Korea Advanced Institute of Science and Technology, Daejeon, South Korea, in 2014 and 2022, respectively. He is currently a Senior Researcher with the Department of Robotics and Mechatronics, Korea Institute of Machinery and Materials (KIMM). His research interests include tendon-driven mechanism, flexible endoscopic surgery robot, two-wheeled legged robot, and soft-exoskeleton using SMA spring.

CHANHUN PARK received the B.S. degree in mechanical engineering from Yeungnam University, Gyeongsan-si, South Korea, in 1994, the M.S. degree in mechanical engineering from POSTECH, Pohang, South Korea, in 1996, and the Ph.D. degree in mechanical engineering from KAIST, Daejeon, South Korea, in 2010. Since 1996, he has been a Principal Researcher with the Department of Robotics and Mechatronics, Korea Institute of Machinery and Materials (KIMM), Daejeon, where he has been the Head of the Department of Robotics and Mechatronics, since 2017. His research interests include robot manipulator design and control, force-feedback control systems, cooperative robot and its application, dexterous manipulators for industrial robotics, gripper systems for human–robot cooperation, and assembly process automation.